

From Noisy to Native: LLM-driven Graph Restoration for Test-Time Graph Domain Adaptation

Xiangwei Lv*
xiangwei.lv@zju.edu.cn
Zhejiang University
Hangzhou, China

JinLuan Yang*
yangjinluan@zju.edu.cn
Zhejiang University
Hangzhou, China

Wang Lin
linwanglw@zju.edu.cn
Zhejiang University
Hangzhou, China

Jingyuan Chen†
jingyuanchen@zju.edu.cn
Zhejiang University
Hangzhou, China

Beishui Liao†
baiseliao@zju.edu.cn
Zhejiang University
Hangzhou, China

Abstract

Graph domain adaptation (GDA) has achieved great attention due to its effectiveness in addressing the domain shift between train and test data. A significant bottleneck in existing graph domain adaptation methods is their reliance on source-domain data, which is often unavailable due to privacy or security concerns. This limitation has driven the development of Test-Time Graph Domain Adaptation (TT-GDA), which aims to transfer knowledge without accessing the source examples. Inspired by the generative power of large language models (LLMs), we introduce a novel framework that reframes TT-GDA as a generative graph restoration problem, “restoring the target graph to its pristine, source-domain-like state”. There are two key challenges: (1) We need to construct a reasonable graph restoration process and design an effective encoding scheme that an LLM can understand, bridging the modality gap. (2) We need to devise a mechanism to ensure the restored graph acquires the intrinsic features of the source domain, even without access to the source data. To ensure the effectiveness of graph restoration, we propose a new approach, named GRAIL, that restores the target graph into a state that is well-aligned with the source domain. Specifically, we first compress the node representations into compact latent features and then use a graph diffusion process to model the graph restoration process. Then a quantization module encodes the restored features into discrete tokens. Building on this, an LLM is fine-tuned as a generative restorer to transform a “noisy” target graph into a “native” one. To further improve restoration quality, we introduce a reinforcement learning (RL) process guided by specialized alignment and confidence rewards. This ensures the restored target graph possesses the key attributes of the source

graph. Extensive experiments demonstrate the effectiveness of our approach across various datasets.

CCS Concepts

• Computing methodologies → Machine learning.

Keywords

Test-Time Graph Domain Adaptation, Generative Graph Restoration, Graph Neural Networks

ACM Reference Format:

Xiangwei Lv, JinLuan Yang, Wang Lin, Jingyuan Chen, and Beishui Liao. 2025. From Noisy to Native: LLM-driven Graph Restoration for Test-Time Graph Domain Adaptation. In *Proceedings of Make sure to enter the correct conference title from your rights confirmation email (Conference acronym 'XX)*. ACM, New York, NY, USA, 10 pages. <https://doi.org/XXXXXXX.XXXXXXX>

1 Introduction

Graph Neural Networks (GNNs) have demonstrated remarkable success in modeling structured data across diverse applications, including social networks [4, 5], citation networks [13], and so on. However, their efficacy relies on the critical assumption that training and test data are independently and identically distributed (i.i.d.), which is rarely met in real-world applications. When a GNN is trained on a specific source domain and deployed to a different target domain, it often experiences a significant performance drop due to domain shift. This shift can be attributed to changes in both feature distributions and graph topology [39]. For example, a GNN trained on a citation graph of older ArXiv papers may struggle with more recent ones [22]. This is because shifts in research interests alter the feature distribution, while the emergence of new fields like deep learning profoundly evolves the graph’s topology.

To mitigate the above problem, **Graph Domain Adaptation (GDA)** has emerged, aiming to transfer knowledge from a labeled source domain to an unlabeled target domain [40]. Most existing GDA methods [3, 30, 39, 42, 46] align the feature spaces of the two domains by relying on direct access to source data. However, this is often impractical due to privacy or intellectual property constraints [2, 11, 12, 22]. This practical barrier has motivated a promising research direction: **Test-time Graph Domain Adaptation (TT-GDA)**, which aims to adapt a pre-trained source model to a target graph at test time, without access to the original source

*Equal Contribution

†Corresponding Author

Permission to make digital or hard copies of all or part of this work for personal or classroom use is granted without fee provided that copies are not made or distributed for profit or commercial advantage and that copies bear this notice and the full citation on the first page. Copyrights for components of this work owned by others than the author(s) must be honored. Abstracting with credit is permitted. To copy otherwise, or republish, to post on servers or to redistribute to lists, requires prior specific permission and/or a fee. Request permissions from permissions@acm.org.
Conference acronym 'XX, Woodstock, NY

© 2025 Copyright held by the owner/author(s). Publication rights licensed to ACM.
ACM ISBN 978-1-4503-XXXX-X/2018/06
<https://doi.org/XXXXXXX.XXXXXXX>

data. Inspired by the success of Large Language Models (LLMs) in text, vision, and multimodal domains [1, 15, 19], we naturally consider how to leverage their powerful generative and reasoning capabilities [8, 16] to facilitate the graph adaptation process. Our core idea is to utilize an LLM to learn the latent structural and stylistic properties of a source domain. This implicit knowledge is then applied to refine a target graph, effectively bridging the domain gap without needing direct access to the source data. However, developing an LLM-driven TT-GDA framework presents two fundamental challenges: (1) **Graph Restoration-based Tokenization**. The first challenge is the fundamental modality gap between the non-Euclidean, topological nature of graphs and the sequential, text-based architecture of LLMs [6, 28]. Simply serializing a graph's nodes and edges into a list is a naive solution that fails to capture the rich, high-order structural information and permutation invariance inherent to graph data. Therefore, the core challenge is to devise an effective tokenization scheme that can transform a graph into discrete semantic tokens, where the sequence itself reflects a valid graph formation or restoration process. (2) **Effective Alignment with Source Characteristics**. The second challenge is guiding the LLM's generation process to faithfully instill the target graph with the latent characteristics of an unseen source domain. It is impractical to deterministically predefine an optimal, source-styled restoration process for target graphs. A straightforward solution is to use the source graph to create pseudo graph restoration sequences for supervised fine-tuning (SFT) of an LLM. However, the LLM trained solely via SFT may not effectively determine if its modifications truly conform to the source style, making it a significant challenge to guarantee the quality of the refined target graph.

To address these challenges, we propose **GRAIL**, a novel framework that leverages a fine-tuned LLM to perform the TT-GDA task via target graph restoration and alignment. The overall approach consists of two phases: (1) Graph Diffusion Trajectory Tokenizer and (2) LLM-based Graph Restoration and Alignment. In phase 1, we first utilize a Q-former-based encoder compresses the variable-sized input graph into a set of fixed and compact latent representations. Then, a graph diffusion model learns the generative process of graph restoration at this latent level, producing a sequence that mirrors the step-by-step restoration of a graph. These continuous latent vectors are then discretized into token IDs via a vector quantizer, preparing the data for the LLM. In phase 2, we fine-tune an LLM on token sequences generated by phase 1 to master the task of graph restoration. To enhance the quality of target graph refinement without source data, we introduce a reinforcement learning algorithm with specialized alignment and confidence rewards, aiming to encourage the LLM to produce a graph that is well-aligned with the latent characteristics of the source domain.

Our contributions are summarized as follows:

- We are the first to formalize and address the problem of Test-Time Graph Domain Adaptation (TT-GDA) by using a Large Language Model to refine the target graph data, eliminating the need for source data during adaptation.
- We propose GRAIL, a novel framework comprising two key components: a graph diffusion trajectory tokenizer that models the graph restoration process and then tokenizes its trajectory for

bridging the modality gap, and a reinforcement learning algorithm that provides effective source-free guidance for graph refinement.

- We conducted comprehensive experiments on multiple benchmarks, which validate the effectiveness of GRAIL by showing it significantly outperforms existing state-of-the-art methods.

2 Related Work

Graph Domain Adaptation (**GDA**) aims to effectively transfer knowledge from a labeled source graph to an unlabeled target graph [18, 31, 40, 47]. Most existing GDA approaches address this challenge through adversarial learning [21, 31, 39] or by minimizing the distributional distance [7, 44] between the source and target graphs, often using metrics like Maximum Mean Discrepancy (MMD). However, these methods heavily rely on direct access to the source graph, which is often infeasible in real-world applications due to privacy, security, or data ownership constraints.

To overcome the limitations of traditional GDA, Test-Time Graph Domain Adaptation (**TT-GDA**) has emerged as a promising research area. While test-time adaptation (TTA) methods have been explored in the vision domain [17, 20, 35], applying them to graph data presents unique challenges due to its complex topological structures and relational dependencies. Existing TT-GDA approaches can be broadly categorized into two main groups based on how they adapt the pre-trained model on source graphs: (1) **Data-Centric Approaches**: These methods primarily focus on modifying or augmenting the input data to facilitate adaptation. For instance, GTrans [11] uses a surrogate loss to guide the adaptation process, while GraphPatcher [12] improves predictions on low-degree nodes by introducing virtual nodes connected to the existing graph. (2) **Model-Centric Approaches**: These approaches directly adjust the learned model's parameters to align with the target domain. For example, SOGA [22] utilizes mutual information maximization and a structure consistency objective to improve the adaptation process. Besides, Matcha [2] proposes adjusting the hop-aggregation parameters of the graph neural network to mitigate the effects of structural domain shifts. Our approach follows the data-centric perspective and creatively uses an LLM to restore the target graph with source characteristics, allowing it to perform well with the pre-trained source model.

3 Preliminaries

3.1 Problem Definition

Given a graph $G = (V, E)$, where V is the set of nodes and E is the set of edges. Let $n = |V|$ and $m = |E|$ denote the total number of nodes and edges, respectively. The graph structure is represented by an adjacency matrix $A \in \{0, 1\}^{n \times n}$, where $A_{ij} = 1$ if an edge exists between node $v_i \in V$ and $v_j \in V$, and $A_{ij} = 0$ otherwise. The feature matrix is represented as $X \in \mathbb{R}^{n \times d}$, where d is the feature dimension. In the context of domain adaptation, we distinguish between a source graph G^s and a target graph G^t . They share the same label space but have different data distributions. The source graph G^s is accompanied by a label matrix $Y \in \{0, 1\}^{n \times C}$, where C is the number of classes. We assume a Graph Neural Network (GNN), denoted as f_{GNN}^s , has been pre-trained on the source graph G^s for a node classification task. The objective of **Test-Time Graph Domain**

Adaptation (TT-GDA) is to effectively improve the performance of the pre-trained model f_{GNN}^s on the target graph G^t . A critical constraint is that the source graph G^s is not accessible during the adaptation process, typically due to privacy concerns.

3.2 Graph Neural Networks

Graph Neural Networks (GNNs) are models designed to process graph data by iteratively aggregating and transforming information from a node's neighbors [13, 38, 38, 43]. This message-passing mechanism updates the feature representation of each node, enabling GNNs to learn powerful node embeddings. A typical GNN layer can be expressed as:

$$h_i^{(l+1)} = \text{UPDATE}^{(l)} \left(h_i^{(l)}, \text{AGG}^{(l)} \left(\{h_j^{(l)} | v_j \in \mathcal{N}(v_i)\} \right) \right) \quad (1)$$

where $h_i^{(l)}$ is the feature vector of node v_i at layer l , and $\mathcal{N}(v_i)$ is the set of neighbors of node v_i . $\text{AGG}^{(l)}$ denote the aggregation function to aggregates the feature vectors from the neighbors. And $\text{UPDATE}^{(l)}$ represent the update to combines the aggregated neighbor information with the node's current features to generate a new representation. After L layers, a final set of node embeddings is obtained for tasks like node classification.

3.3 Diffusion Models

Diffusion models have become a prominent class of generative models, achieving significant progress in computer vision and other domains [24, 25, 45]. They are primarily composed of two core phases: a forward diffusion process and a reverse denoising process.

Given a data distribution $p(\mathbf{x}_0)$, the forward process gradually adds Gaussian noise to the data. This is modeled as a Markov chain where, at each step t , the transition from \mathbf{x}_{t-1} to \mathbf{x}_t is defined by the following distribution:

$$q(\mathbf{x}_t | \mathbf{x}_{t-1}) = \mathcal{N}(\mathbf{x}_t; \sqrt{1 - \beta_t} \mathbf{x}_{t-1}, \beta_t \mathbf{I}) \quad (2)$$

Here, $\beta_t \in (0, 1)$ is a predefined variance schedule that controls the amount of noise added at step t , and \mathbf{I} is the identity matrix. A key property of this process is that we can directly sample \mathbf{x}_t from the initial data point \mathbf{x}_0 without needing the intermediate steps. This is made possible by the reparameterization trick, which yields the following relationship:

$$\mathbf{x}_t = \sqrt{\bar{\alpha}_t} \mathbf{x}_0 + \sqrt{1 - \bar{\alpha}_t} \epsilon_t \quad (3)$$

where $\alpha_t = 1 - \beta_t$, $\bar{\alpha}_t = \prod_{i=1}^t \alpha_i$, and $\epsilon_t \sim \mathcal{N}(\mathbf{0}, \mathbf{I})$ is a standard Gaussian noise vector.

The reverse process aims to train a neural network, parameterized by θ , to model the reverse transitions $p_\theta(\mathbf{x}_{t-1} | \mathbf{x}_t)$. This learned process progressively removes the noise added in the forward process to generate new data. Similar to the forward transitions, the reverse transition is also modeled as a Gaussian distribution:

$$p_\theta(\mathbf{x}_{t-1} | \mathbf{x}_t) = \mathcal{N}(\mathbf{x}_{t-1}; \mu_\theta(\mathbf{x}_t, t), \Sigma_\theta(\mathbf{x}_t, t)) \quad (4)$$

where $\mu_\theta(\mathbf{x}_t, t)$ and $\Sigma_\theta(\mathbf{x}_t, t)$ represent the predicted mean and covariance of the reverse distribution, respectively. In the Denoising Diffusion Probabilistic Models (DDPM) framework [10], the covariance is often fixed to a small constant, such as $\Sigma_\theta(\mathbf{x}_t, t) = \beta_t \mathbf{I}$. The $\mu_\theta(\mathbf{x}_t, t)$ is learned by the neural network, can be derived through

reparameterization trick as:

$$\mu_\theta(\mathbf{x}_t, t) = \frac{1}{\sqrt{\alpha_t}} \left(\mathbf{x}_t - \frac{\beta_t}{\sqrt{1 - \bar{\alpha}_t}} \epsilon_\theta(\mathbf{x}_t, t) \right) \quad (5)$$

where $\epsilon_\theta(\mathbf{x}_t, t)$ denote the noise prediction network, which can be implemented through neural networks. Finally, the mean squared error is used as objective loss to train $\epsilon_\theta(\mathbf{x}_t, t)$ by:

$$\mathcal{L} = \mathbb{E}_{t, \mathbf{x}_0, \epsilon_t} [\|\epsilon_t - \epsilon_\theta(\mathbf{x}_t, t)\|^2] \quad (6)$$

4 Method

4.1 Overview

In this section, we propose GRAIL, a novel method that leverages Large Language Models (LLMs) to perform graph restoration and effectively align a target graph with source-domain characteristics. As illustrated in Figure 1, our approach comprises two key stages: (1) **Graph Diffusion Trajectory Tokenizer**, (2) **LLM-based Graph Restoration and Alignment**. In **stage 1**, we aim to obtain desired restored graph sequences and effectively encode them into token IDs for subsequent LLM training. To achieve this, we first introduce a Q-Former framework to compress a variable number of nodes into a fixed and compact set of latent representations. A diffusion model is then trained on these latent features through a forward noise-adding process and a reverse denoising process. To further map these latent representations into tokens, we incorporate a quantizer to discretize the continuous representations. Finally, a decoder is employed to reconstruct the graph data to mitigate information loss. In **stage 2**, We first leverage the diffusion model trained in Stage 1 to generate graph sequences that simulate the graph restoration process. These generated sequences are subsequently tokenized into discrete token streams. We then employ an LLM to model this restoration process in an autoregressive manner. To overcome the limitations of simple imitation learning, we further enhance the model through a reinforcement learning process. This stage guides the LLM to discover implicit source characteristics and perform graph refinements by using a dual-component reward function, which includes an alignment reward and a confidence reward.

4.2 Graph Diffusion Trajectory Tokenizer

As mentioned, our aim is to model the evolution of graph restoration to capture the inherent source characteristics so that we can refine the target graph for improved adaptation. Due to the complex and variable topology of graphs, we propose to first encodes them into manageable embeddings, which then undergo a diffusion process. These embeddings can then transformed into discrete tokens to serve as the basic units for training an LLM. Since our primary focus is on node classification, we use the subgraph G_u^s centered at node $u \in V$ as our initial input. We detail more components below. **Encoder.** We first utilize a trained GNN f_{GNN}^s to obtain node representations $H \in \mathbb{R}^{p \times d}$. Since the number of nodes p can vary for each sampled subgraph, we need a way to process these variable-sized representations. Inspired by the Q-Former's use in computer vision [33]—where it employs learnable query embeddings to build interactions between text and visual data—we adopt a similar strategy. Specifically, we employ K learnable query tokens $Q \in \mathbb{R}^{K \times d}$ to obtain a fixed-size, compact latent representation. The Q-Former

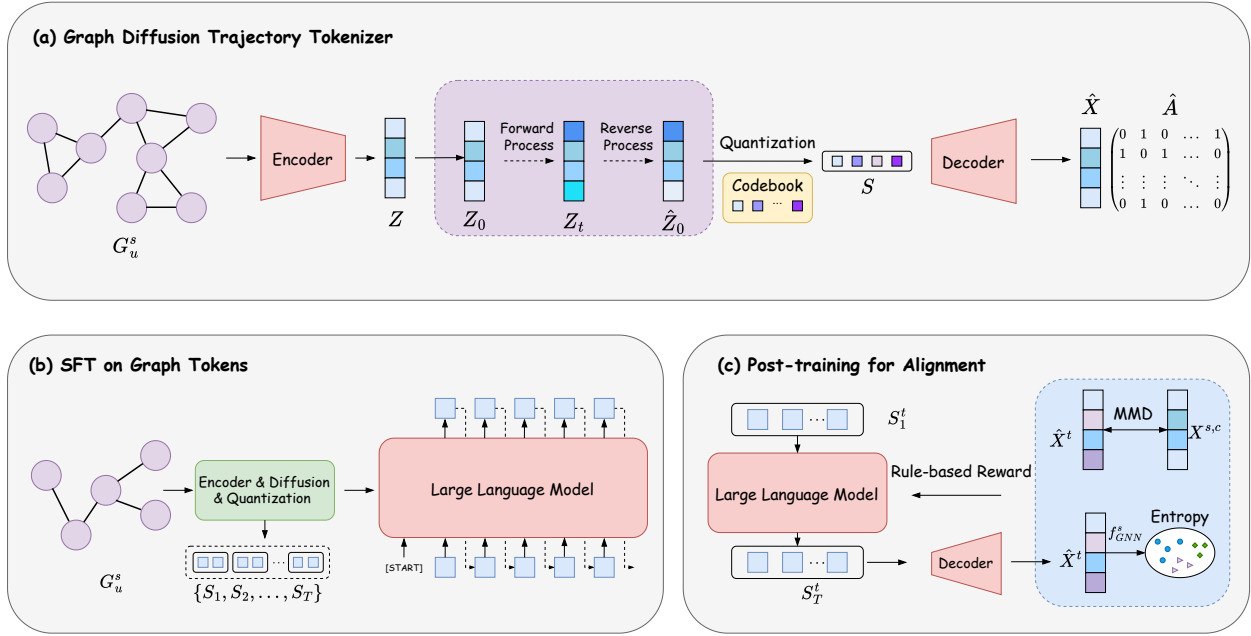


Figure 1: The architecture of GRAIL. (a) *Graph Diffusion Trajectory Tokenizer* utilizes a graph diffusion process to create a source graph restoration trajectory at the embedding level. The trajectory is subsequently tokenized into discrete token IDs. An additional decoder then reconstructs the graph from these tokenized ids. (b) *SFT on Graph Tokens* uses the tokenized sequences from stage (a) to fine-tune an LLM, which enables the LLM to understand and model the graph restoration process in an autoregressive manner. (c) *Post-training for Alignment* further enhances the LLM’s restoration capabilities by incorporating a reinforcement learning process, which leverages alignment and confidence rewards to refine target graphs with source characteristics.

processes these tokens through a series of operations:

$$Q' = \text{SelfAttn}(Q) \quad (7)$$

$$H_Q = \text{CrossAttn}(Q'; H) \quad (8)$$

$$Z = \text{MLP}(H_Q) \quad (9)$$

Here, **SelfAttn** is the self-attention operation [37] that allows the query tokens to interact with each other, capturing their internal relationships to obtain $Q' \in \mathbb{R}^{K \times d}$. The **CrossAttn** means the cross attention operation, which enables the refined query tokens to extract a fixed-size representation, $H_Q \in \mathbb{R}^{K \times d}$. Finally, a multi-layer perceptron (MLP) is employed to obtain the final compressed representation $Z \in \mathbb{R}^{K \times d}$. This representation provides a standardized input for subsequent diffusion model operations.

Diffusion Process. Given that the diffusion process is designed to reconstruct original information from corrupted data [21, 45], we utilize a diffusion model to capture source characteristics and subsequently employ it for constructing restoration sequences. We model the graph restoration process on source graph using a diffusion framework as follows:

$$Z \rightarrow Z_0 \xrightarrow{\phi} Z_1 \xrightarrow{\phi} \dots \xrightarrow{\phi} Z_t \xrightarrow{\psi} \hat{Z}_{t-1} \xrightarrow{\psi} \dots \xrightarrow{\psi} \hat{Z}_0 \quad (10)$$

where ϕ and ψ denote the adding noise and removing noise process. Followed Equation 6, the training objective of diffusion is

formally as:

$$\mathcal{L}_{diff} = \mathbb{E}_{t, Z_0, \epsilon_t} [\|\epsilon_t - \epsilon_\theta(Z_t, t)\|^2] \quad (11)$$

After training, we can construct a sequence of restored embeddings at the embedding level, denoted as $Z_{res} = \{Z_T, Z_{T-1}, \dots, Z_0\}$, where T is the total restoration steps. This sequence effectively tracks the restoration process from a corrupted representation back to the original characteristics.

Quantizer. Our objective is to leverage LLMs to comprehend and effectively address the graph restoration process. However, the continuous nature of the embedding sequence Z_{res} is fundamentally incompatible with the discrete, token-based generation and reasoning capabilities of LLMs. To bridge this representational gap, we incorporate a quantization strategy to discretize these continuous representations [14, 26, 27]. Specifically, we maintain a learnable codebook, $P = \{p_i\}_{i=1}^M$, where M is the codebook size and each $p_i \in \mathbb{R}^d$ is a learnable embedding vector. The quantization process transforms each continuous embedding $Z_{t,i}$ (the i -th row vector of Z_t) into its nearest discrete token s_t . This is achieved by finding the index of the closest vector in the codebook P in terms of Euclidean distance:

$$s_{t,i} = \underset{j \in \{1, \dots, M\}}{\operatorname{argmin}} \|Z_{t,i} - p_j\|_2 \quad (12)$$

Through this operation, the each continuous embedding sequence Z_t is transformed into a discrete token sequence, $S_t = \{s_{t,K}, \dots, s_{t,0}\}$, which can be seamlessly processed by an LLM.

Decoder. The decoder is responsible for reconstructing the graph from the compressed discrete tokens S produced by the encoder and quantizer. Its primary goal is to invert the quantization process and encoder process while preserving the integrity of the latent information. The decoder first maps the discrete token sequence S back into a continuous latent space through looking up the corresponding embeddings from the codebook P , yielding the de-quantized embedding $\hat{Z} \in \mathbb{R}^{K \times d}$:

$$\hat{Z} = \text{Lookup}(S; P) \quad (13)$$

Similar to the encoder, the decoder employs a Q-former framework to reconstruct the representation. It utilizes query vectors $Q_{dec} \in \mathbb{R}^{p \times d}$, which are generated through $Q_{dec} = \text{MLP}(X)$. This approach allows the decoder to leverage the original graph's characteristics to guide the reconstruction. Furthermore, the decoding process involves a cross-attention mechanism where the dynamic queries Q_{dec} interact with the de-quantized embedding \hat{Z} (serving as key and value):

$$H_{rec} = \text{CrossAttn}(Q_{dec}; \hat{Z}) \quad (14)$$

The final node features and adjacency matrix are reconstructed as follows:

$$\hat{X} = \text{MLP}(H_{rec}) \quad (15)$$

$$\hat{A}_{ij} = \sigma(H_{rec,i}^\top H_{rec,j}) \quad (16)$$

where σ is the sigmoid function. This structured process ensures the decoder can accurately restore both the node features and the graph's topological structure from the compressed latent space.

Training. We adopt an end-to-end training approach driven by a composite loss function, ensuring that each component contributes to the final graph restoration task. The total loss function is defined as:

$$\mathcal{L}_{total} = \mathcal{L}_{diff} + \lambda_1 \mathcal{L}_{quant} + \lambda_2 \mathcal{L}_{dec} \quad (17)$$

where λ_1, λ_2 are hyperparameters controlling the weight of each loss term.

- **Quantization Loss (\mathcal{L}_{quant}):** This loss ensures the continuous embeddings from the encoder can be effectively mapped to the discrete codebook. It combines a reconstruction term and a commitment term to stabilize training:

$$\mathcal{L}_{quant} = \|\text{sg}[Z] - p_s\|_2^2 + \|Z - \text{sg}[p_s]\|_2^2 \quad (18)$$

$$\text{where } p_{s,i} = \arg \min_{c \in P} \|Z_i - c\|_2^2 \quad (19)$$

Here, $\text{sg}[\cdot]$ is the stop-gradient operator. The first term pulls the codebook vectors (p_s) toward the encoder outputs (Z), while the second term pulls the encoder outputs toward the codebook vectors, preventing the embeddings from collapsing.

- **Decoding Loss (\mathcal{L}_{dec}):** This loss guarantees the decoder can accurately reconstruct the original graph from the processed latent representation. It consists of two parts: a Binary Cross-Entropy (BCE) loss for the adjacency matrix and an L2 loss for the node features:

$$\mathcal{L}_{dec} = \text{BCE}(\hat{A}, A) + \|\hat{X} - X\|_2^2 \quad (20)$$

4.3 LLM-driven Graph Alignment

4.3.1 LLM Pre-training on Graph Tokens. With trained diffusion process and quantizer model, we can transform graph restoration process into discrete token sequences that LLM can understand like language. The transferred token symbols are viewed as new tokens needed to further learn. To enable the LLM to master the graph restoration process, we first extend its vocabulary by introducing M new tokens. We then fine-tune the LLM to maximize the likelihood of the graph restoration process in an autoregressive manner. Formally, given a sequence of graph $\{S_1, S_2, \dots, S_T\}$ tokens obtained from the diffusion process, where each $S_i = \{s_{i,1}, s_{i,2}, \dots, s_{i,K}\}$, the fine-tuning objective is to minimize the negative log-likelihood as follows:

$$\mathcal{L}_{LLM} = -\frac{1}{T \cdot K} \sum_{i=1}^T \sum_{j=1}^K \log P(s_{i,j} | S_{<i}, s_{i,<j}) \quad (21)$$

where $S_{<i}$ represents the entire sequence of tokens from all previous restoration steps (S_1, S_2, \dots, S_{i-1}). $s_{i,<j}$ represents the sequence of tokens from the current step i that have already been generated ($s_{i,1}, s_{i,2}, \dots, s_{i,j-1}$). In this way, LLM will learn how to generate needed graph tokens to represent graph characteristics.

4.3.2 Post-Training for Source Alignment. To enhance the alignment of graph tokens generated by our LLM with the implicit characteristics of the source domain, we employ reinforcement learning (RL) fine-tuning. This approach, inspired by reasoning models, guides the LLM to capture and restore the implicit properties of the source data during the graph refinement process.

Here, we utilize Group Relative Policy Optimization (GRPO) [8] for fine-tuning. Unlike standard RL algorithms that rely on a separate critic model like PPO [29], GRPO directly leverages a group of candidate responses to estimate the advantage. Given an input refined graph \hat{G}^t , GRPO first samples g distinct output sequences $\{o_1, o_2, \dots, o_g\}$ from the old policy π_{old} and computes their corresponding rewards $\{r_1, r_2, \dots, r_g\}$. The advantage A_i for each output o_i is then computed by normalizing its reward against the batch statistics:

$$A_i = \frac{r_i - \text{mean}(\{r_1, \dots, r_g\})}{\text{std}(\{r_1, \dots, r_g\})} \quad (22)$$

where mean and std represent the mean and standard deviation of the reward group, respectively.

The RL objective is defined to maximize the expected reward while penalizing large policy shifts, ensuring stable training:

$$\max_{\pi_\theta} \mathbb{E}_{o \sim \pi_\theta(\hat{G}^t)} [R(\hat{G}^t, o) - \beta \mathbb{D}_{KL}[\pi_\theta(o | \hat{G}^t) || \pi_{old}(o | \hat{G}^t)]] \quad (23)$$

where \mathbb{D}_{KL} is the KL-divergence, a measure of policy divergence, and β is a hyperparameter that controls the weight of the KL penalty. $R(\hat{G}^t, o)$ is the reward function.

We design a composite reward function to guide the LLM's refinement process, comprising two main components: an alignment reward and a confidence reward. The alignment reward, R_{align} , ensures that the generated graph's node embedding distribution statistically aligns with that of the source domain. We use Maximum Mean Discrepancy (MMD) as our metric [7, 32], which measures the

distance between two probability distributions in a reproducing kernel Hilbert space. The squared MMD distance, d_{MMD}^2 , is calculated between two sets of node embeddings: one from the refined graph and one from the original source graph. Given the constraints of the TT-GDA task, we cannot directly access the source domain data. To address this, we maintain a cluster centroid matrix, $X^{s,c} \in \mathbb{R}^{C \times d}$, as a statistical representation of the source domain. This is computed by simply averaging the vectors within each class. In this manner, we obtain an approximate distribution of the source domain without explicitly accessing the source data. Let \hat{X}^t be the sets of node embeddings for the refined graph with C' nodes. The squared MMD distance is calculated as follows:

$$d_{MMD}^2 = \frac{1}{C'(C'-1)} \sum_{i \neq j}^{n_1} k(\hat{X}_i^t, \hat{X}_j^t) + \frac{1}{C(C-1)} \sum_{i \neq j}^{n_2} k(X_i^{s,c}, X_j^{s,c}) - \frac{2}{CC'} \sum_{i=1}^{C'} \sum_{j=1}^C k(\hat{X}_i^t, X_j^{s,c}) \quad (24)$$

where $k(\cdot, \cdot)$ is a kernel function, such as the Gaussian kernel, which computes the similarity between node embeddings. To convert this distance into a reinforcement learning signal, we define the alignment reward as:

$$R_{align} = e^{-\gamma d_{MMD}^2} \quad (25)$$

where $\gamma > 0$ is a hyperparameter that controls the reward decay rate. This formulation ensures that $R_{align} \in (0, 1]$, providing a stable and well-bounded reward signal.

As a gold standard for downstream performance is unavailable, we instead use the prediction confidence of a pre-trained GNN model f_{GNN}^s as a proxy for the quality of the refined graph. We define the downstream reward as the average negative entropy of the GNN's predictions on the refined graph. The reward is calculated based on predicted probabilities of f_{GNN}^s for each node in the refined graph \hat{G}^t :

$$R_{conf} = -\frac{1}{C'} \sum_{i=1}^{C'} \sum_{c=1}^C p_{i,c} \log p_{i,c} \quad (26)$$

where $p_{i,c}$ denotes the probability of node i belonging to class c . Maximizing this reward encourages the LLM to generate graphs that lead to more confident predictions by the downstream GNN, thereby improving its performance on the target domain. Consequently, the final reward function for a generated graph is a composite of the two defined rewards:

$$R_{final} = R_{align} + R_{conf} \quad (27)$$

This dual-component reward guides the model to both align its output with source characteristics and improve the predictive confidence of the refined graph.

5 Experiments

We conduct comprehensive experiments to address the following key research questions:

- RQ1: Does our proposed method achieve significant performance improvements on the node-level Test-Time Graph Domain Adaptation task?
- RQ2: Do the various components of our proposed approach each contribute to the final performance?
- RQ3: What is the impact of our approach on the quality of target graph refinement?
- RQ4: How does the proposed method's performance vary with key hyperparameters, such as the loss weight λ_1, λ_2 , codebook size M and refinement steps T ?

Table 1: Statistics of the datasets.

Datasets	#Nodes	#Edges	#Features	#Labels
DBLPv7	5,484	4412	6,755	5
ACMv9	9,360	15,602	6,775	5
Citationv1	8,935	5379	6,755	5

5.1 Experiment Settings

Datasets. For our experiments, we follow prior work [23, 39] and utilize three widely adopted real-world network datasets from the **ArnetMiner** collection [34]: ACMv9, Citationv1, and DBLPv7. These three datasets are citation networks from distinct sources and time periods: ACMv9 (after 2010), Microsoft Academic Graph (before 2008), and DBLP (from 2004 to 2008). We represent each network as an undirected graph, where each node corresponds to a paper and an edge signifies a citation relationship between two papers. Each paper is assigned to one of five research categories: *Artificial Intelligence*, *Computer Vision*, *Database*, *Information Security*, and *Networking*. For simplicity, these datasets are denoted as A, C, and D, respectively. Due to their distinct sources and collection periods, these datasets exhibit significant differences in both feature distributions and topological structures, making them ideal for evaluating domain adaptation methods. A detailed statistical overview of these datasets is provided in Table 1.

Baselines. We mainly consider the following baseline TT-GDA methods for comparison:

- **Vanilla GNN Methods:** This category includes standard GNN models such as GCN [13], GSAGE [9], and GAT [38]. These models are trained on the source graph and then directly evaluated on the target graph without any adaptation, serving as a performance lower bound.
- **Model-Centric TT-GDA Methods:** These approaches focus on adjusting the pre-trained model's parameters to improve adaptation. We include EERM [41], SOGA [22], and Matcha [2] in this group. They typically employ different self-supervised loss functions or unique architectural designs to achieve adaptation.
- **Data-Centric TT-GDA Methods:** These methods, represented by GTrans [11] and GraphPatcher [12], aim to modify the target graph itself to better align it with the source graph's distribution. This allows the pre-trained GNN to perform better without needing to alter its parameters.

Metrics. We evaluate our model's performance on the target graph using the Micro-F1 and Macro-F1 scores for classification.

Implementation Details. We select the GCN as the default source-trained GNN model, denoted as f_{GNN}^s . For a fair comparison, we

set the hidden size for both our method and all baselines to 256. For the training of our encoder and diffusion model, we randomly sample source subgraphs up to their 3-hop neighbors. The number of learnable query tokens K is set to 128. The number of denoising steps for the diffusion process, T , is set to 10, and the codebook size, C , is 128. The loss weights λ_1 and λ_2 are configured as 0.4 and 1.0, respectively. In the LLM-driven graph alignment stage, we utilize the Llama3.1-8B as our base pre-trained model. The learning rates for SFT and subsequent reinforcement learning processes are set to 1×10^{-4} and 2×10^{-6} , respectively.

5.2 Main Results (RQ1)

As shown in Table 2, our approach consistently outperforms all baseline methods across every TT-GDA scenario. For instance, our method achieves an average 2.04% improvement in the Macro-F1 score. This demonstrates that our method effectively leverages LLMs to refine graphs and imbue the target graph with latent source characteristics, leading to superior performance. Overall, Both model-centric and data-centric TT-GDA methods generally outperform vanilla GNNs, highlighting the inherent challenge of this task and the necessity for specialized solutions. The data-centric approaches, in particular, appear to achieve better overall performance than the model-centric ones. Our method, which is a data-centric approach, significantly surpasses existing alternatives in this category. This superior performance can be attributed to several key factors: Our method combines a diffusion process with an LLM, treating the graph as a sequence of tokens. This enables a more powerful restoration process, as the LLM can generate a refined graph structure and node features that are more effectively aligned with the source domain. We introduced a reinforcement learning process that effectively enhances the quality of the target graph’s refinement. This is achieved through specially designed alignment and confidence rewards, which provide a clear feedback signal to the LLM. This guidance encourages the LLM to make more effective changes, ultimately improving performance on the target domain.

5.3 Ablation Studies (RQ2)

To assess the contribution of each component in our method, we conduct extensive experiments comparing the following variants:

- **w/o Encoder:** This variant removes the Q-former design and instead randomly selects a fixed number of nodes as the initial input for the diffusion process.
- **w/o Diff:** This variant omits the diffusion process. It instead constructs the graph restoration sequences by randomly removing or adding edges.
- **w/o Align:** This variant removes the alignment reward, which is based on the MMD distance.
- **w/o Conf:** This variant removes the confidence reward, which is based on entropy calculation.

As illustrated in Figure 2, the performance degradation of the **w/o Encoder** variant shows that our Q-former-based encoder effectively encodes a variable number of nodes into a fixed, compact latent representation for subsequent training. The performance drop observed in the **w/o Diff** variant demonstrates that the diffusion process is effective at modeling the graph restoration process,

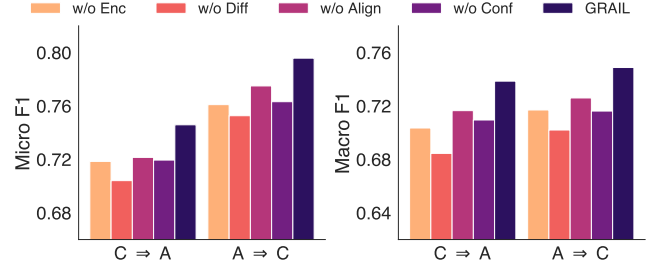


Figure 2: Ablation studies on $C \Rightarrow A$ and $A \Rightarrow C$.

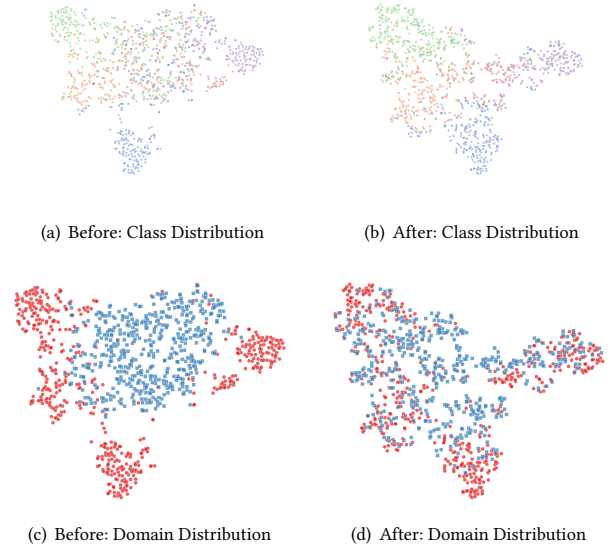


Figure 3: Visualization of node embeddings on the $C \Rightarrow A$ domain adaptation task. (a) and (b) show the node distributions colored by their *class labels* before and after refining target subgraph, respectively. (c) and (d) show the node distributions colored by their *domain type* (source or target) before and after refining.

which is crucial for recovering source characteristics. This forms a solid foundation for the subsequent LLM fine-tuning and post-training steps. Furthermore, GRAIL’s superior performance over the **w/o Align** and **w/o Conf** variants highlights the effectiveness of our designed rewards in the reinforcement learning phase. The alignment reward ensures the refined target graph maintains statistical properties aligned with the source domain, while the confidence reward prevents the refinement process from sacrificing quality for the sake of simply increasing alignment, thereby ensuring the integrity of the final graph.

5.4 Effectiveness of Refined Target Graph (RQ3)

We further compare the representation distribution of the original target graph and the adapted target subgraph. We employ t-SNE [36] to project the learned latent representations into a 2-dimensional space, as shown in Figure 3. First, we use colors to

Table 2: The performance (%) of all models is evaluated across six domain adaptation scenarios. The best results are highlighted and the second-best results are underlined.

Methods	$C \Rightarrow A$		$D \Rightarrow A$		$A \Rightarrow C$		$D \Rightarrow C$		$A \Rightarrow D$		$C \Rightarrow D$	
	Micro	Macro	Micro	Macro	Micro	Macro	Micro	Macro	Micro	Macro	Micro	Macro
GCN	65.15	64.11	58.68	53.35	72.46	64.34	69.37	66.10	65.27	61.80	66.52	64.24
GSAGE	62.34	60.73	52.13	51.67	66.31	64.10	68.13	65.73	63.12	60.09	65.17	63.19
GAT	64.15	62.25	57.23	54.50	73.01	65.23	70.14	67.10	66.82	65.78	66.12	65.43
EERM	69.73	67.87	68.94	68.73	74.75	70.20	74.12	72.42	68.66	65.37	67.86	67.28
SOGA	70.19	68.15	<u>70.61</u>	69.28	76.90	70.31	76.73	74.04	67.42	66.61	68.58	68.58
Matcha	70.49	69.03	70.48	<u>69.33</u>	<u>77.46</u>	71.31	77.20	75.71	68.36	68.05	70.22	69.73
GTrans	71.91	70.40	69.72	68.37	77.18	71.22	76.13	75.93	69.61	68.37	70.24	70.07
GraphPatcher	<u>72.38</u>	<u>71.03</u>	70.17	69.09	77.09	<u>72.34</u>	<u>77.90</u>	<u>75.94</u>	<u>70.12</u>	<u>69.88</u>	<u>71.99</u>	<u>72.82</u>
GRAIL	74.59	73.86	72.19	71.07	79.58	74.88	79.49	77.75	71.64	71.93	74.37	74.11
Improv.(%)	+2.21	+2.83	+1.71	+1.74	+2.12	+2.54	+1.59	+1.81	+1.52	+2.05	+2.38	+1.29

represent the class labels and visualize the embedding distributions before and after adaptation in Figures 3(a) and (b). We observe that the distribution in (b) is more distinct and well-separated, with a notably better clustering of points in the central region compared to the mixed distribution in (a). This demonstrates that our graph refinement process effectively improves the source model’s performance on the target graph by enhancing class separability.

Furthermore, in Figures 3(c) and (d), we use color to differentiate the domains (blue for source and red for target). Through these visualizations, we observe that the adapted target nodes are better aligned with the source nodes in (d), forming a more cohesive cluster. In contrast, as shown in (c), the initial target nodes exhibit a more discrete and separate distribution from the source nodes. This successful alignment can be attributed to our introduced diffusion process and the alignment reward design, which together enable the generation of a refined target graph with latent source characteristics.

5.5 Hyperparameters Analysis (RQ4)

Table 3: Impact of codebook size M .

M		32	64	128	256	512
$C \Rightarrow A$	Micro	72.1	73.22	74.59	74.12	73.01
	Macro	71.12	73.15	73.86	73.60	73.17
$A \Rightarrow C$	Micro	78.83	79.45	79.85	79.90	79.12
	Macro	74.17	74.72	74.88	74.60	73.92

To further analyze the effectiveness and robustness of our approach, we conducted a thorough investigation into the impact of several key hyperparameters. We investigate the influence of the weight parameters λ_1 and λ_2 (defined in Equation 17) on our model’s performance. The results of this analysis are presented in Figure 4. The weight λ_1 controls the importance of the quantization loss. As demonstrated by the results, the model’s performance

Table 4: Impact of restoration steps T .

T		2	5	10	20	30
$C \Rightarrow A$	Micro	72.1	74.59	73.19	72.12	71.81
	Macro	71.12	73.86	73.86	72.60	70.17
$A \Rightarrow C$	Micro	78.83	79.85	77.90	75.90	73.12
	Macro	73.17	74.88	74.10	73.60	72.17

first improves as λ_1 increases and then begins to decrease slowly. This suggests that the quantization loss is crucial for ensuring the discrete representations retain sufficient information for the LLM’s predictive task. However, an overemphasis on this loss can diminish the effect of the primary diffusion loss, leading to a performance drop. Besides, the performance for λ_2 remains relatively stable across the range of $[0, 1]$. Given this stability, we set $\lambda_2 = 1$ as our default for simplicity, ensuring a consistent contribution from this term. For the codebook size M , a larger codebook can capture more intricate details but also increases the number of learnable parameters, placing a greater burden on the LLM during inference. As shown in Table 3, a codebook size of $M = 128$ strikes an optimal balance. We also analyze the impact of the number of restoration steps T , on performance, as shown in Table 4. A maximum number of steps was set to prevent unbounded generation. Experiments show that a relatively small number of steps, such as $T = 5$, is sufficient. Performance begins to decrease beyond this point. This may be attributed to error accumulation, as the LLM’s sequential reasoning over more steps can degrade the quality of the final graph restoration.

6 Conclusion

This paper introduces GRAIL, a novel framework for Test-time Graph Domain Adaptation (TT-GDA). Addressing a key limitation of traditional methods, GRAIL leverages a fine-tuned Large Language Model (LLM) to refine target graphs without access to source

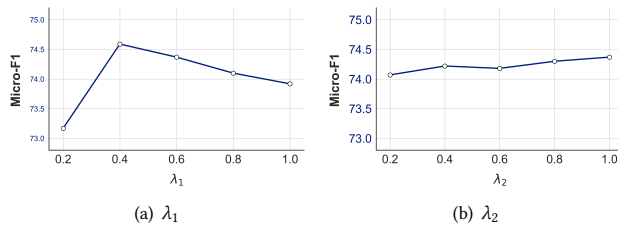


Figure 4: Micro-F1 of various weight parameters.

data. Our core contributions lie in solving two fundamental challenges: bridging the modality gap between graphs and text, and providing effective source-free guidance. To bridge the modality gap, we propose a novel graph diffusion-based tokenization scheme, which transforms complex graph structures into learnable discrete tokens for the LLM. For source-free guidance, we introduce a reinforcement learning algorithm with specialized alignment and confidence rewards, ensuring the refined graphs align with the target domain's latent characteristics. Comprehensive experiments on various datasets validate GRAIL's effectiveness, demonstrating its superior performance over state-of-the-art methods.

References

- [1] Josh Achiam, Steven Adler, Sandhini Agarwal, Lama Ahmad, Ilge Akkaya, Florencia Leoni Aleman, Diogo Almeida, Janko Altmenschmidt, Sam Altman, Shyamal Anadkat, et al. 2023. Gpt-4 technical report. *arXiv preprint arXiv:2303.08774* (2023).
- [2] Wenxuan Bao, Zhichen Zeng, Zhining Liu, Hanghang Tong, and Jingrui He. 2024. Matcha: Mitigating Graph Structure Shifts with Test-Time Adaptation. *arXiv preprint arXiv:2410.06976* (2024).
- [3] Quanyu Dai, Xiao-Ming Wu, Jiaren Xiao, Xiao Shen, and Dan Wang. 2022. Graph transfer learning via adversarial domain adaptation with graph convolution. *IEEE Transactions on Knowledge and Data Engineering* 35, 5 (2022), 4908–4922.
- [4] Alex Davies and Nirav Ajmeri. 2022. Realistic synthetic social networks with graph neural networks. *arXiv preprint arXiv:2212.07843* (2022).
- [5] Wenqi Fan, Yao Ma, Qing Li, Yuan He, Eric Zhao, Jiliang Tang, and Dawei Yin. 2019. Graph neural networks for social recommendation. In *The world wide web conference*. 417–426.
- [6] Bahare Fatemi, Jonathan Halcrow, and Bryan Perozzi. 2023. Talk like a graph: Encoding graphs for large language models. *arXiv preprint arXiv:2310.04560* (2023).
- [7] Arthur Gretton, Karsten M Borgwardt, Malte J Rasch, Bernhard Schölkopf, and Alexander Smola. 2012. A kernel two-sample test. *The Journal of Machine Learning Research* 13, 1 (2012), 723–773.
- [8] Daya Guo, Dejian Yang, Haowei Zhang, Junxiao Song, Ruoyu Zhang, Runxin Xu, Qihao Zhu, Shirong Ma, Peiyi Wang, Xiao Bi, et al. 2025. Deepseek-r1: Incentivizing reasoning capability in llms via reinforcement learning. *arXiv preprint arXiv:2501.12948* (2025).
- [9] Will Hamilton, Zhitaoying, and Jure Leskovec. 2017. Inductive representation learning on large graphs. *Advances in neural information processing systems* 30 (2017).
- [10] Jonathan Ho, Ajay Jain, and Pieter Abbeel. 2020. Denoising diffusion probabilistic models. *Advances in neural information processing systems* 33 (2020), 6840–6851.
- [11] Wei Jin, Tong Zhao, Jiayuan Ding, Yozen Liu, Jiliang Tang, and Neil Shah. 2022. Empowering graph representation learning with test-time graph transformation. *arXiv preprint arXiv:2210.03561* (2022).
- [12] Mingxuan Ju, Tong Zhao, Wenhao Yu, Neil Shah, and Yanfang Ye. 2023. Graph-patcher: mitigating degree bias for graph neural networks via test-time augmentation. *Advances in Neural Information Processing Systems* 36 (2023), 55785–55801.
- [13] Thomas N Kipf and Max Welling. 2016. Semi-supervised classification with graph convolutional networks. *arXiv preprint arXiv:1609.02907* (2016).
- [14] Yoonhyung Lee, Younhyung Chae, and Kyomin Jung. 2024. Leveraging VQ-VAE tokenization for autoregressive modeling of medical time series. *Artificial Intelligence in Medicine* 154 (2024), 102925.
- [15] Junnan Li, Dongxu Li, Silvio Savarese, and Steven Hoi. 2023. Blip-2: Bootstrapping language-image pre-training with frozen image encoders and large language models. In *International conference on machine learning*. PMLR, 19730–19742.
- [16] Zhong-Zhi Li, Duzhen Zhang, Ming-Liang Zhang, Jiaxin Zhang, Zengyan Liu, Yuxuan Yao, Haotian Xu, Junhao Zheng, Pei-Jie Wang, Xiuyi Chen, et al. 2025. From system 1 to system 2: A survey of reasoning large language models. *arXiv preprint arXiv:2502.17419* (2025).
- [17] Jian Liang, Ran He, and Tieniu Tan. 2025. A comprehensive survey on test-time adaptation under distribution shifts. *International Journal of Computer Vision* 133, 1 (2025), 31–64.
- [18] Shuhan Liu and Kaize Ding. 2024. Beyond Generalization: A Survey of Out-Of-Distribution Adaptation on Graphs. *arXiv preprint arXiv:2402.11153* (2024).
- [19] Yixin Liu, Kai Zhang, Yuan Li, Zhiling Yan, Chujie Gao, Ruoxi Chen, Zhengqing Yuan, Yue Huang, Hanchi Sun, Jianfeng Gao, et al. 2024. Sora: A review on background, technology, limitations, and opportunities of large vision models. *arXiv preprint arXiv:2402.17177* (2024).
- [20] Jing Ma. 2024. Improved self-training for test-time adaptation. In *Proceedings of the IEEE/CVF Conference on Computer Vision and Pattern Recognition*. 23701–23710.
- [21] Massimiliano Mancini, Samuel Rota Buló, Barbara Caputo, and Elisa Ricci. 2019. Adagraph: Unifying predictive and continuous domain adaptation through graphs. In *Proceedings of the IEEE/CVF Conference on Computer Vision and Pattern Recognition*. 6568–6577.
- [22] Haitao Mao, Lun Du, Yujia Zheng, Qiang Fu, Zelin Li, Xu Chen, Shi Han, and Dongmei Zhang. 2024. Source free graph unsupervised domain adaptation. In *Proceedings of the 17th ACM International Conference on Web Search and Data Mining*. 520–528.
- [23] Haitao Mao, Lun Du, Yujia Zheng, Qiang Fu, Zelin Li, Xu Chen, Shi Han, and Dongmei Zhang. 2024. Source free graph unsupervised domain adaptation. In *Proceedings of the 17th ACM International Conference on Web Search and Data Mining*. 520–528.
- [24] Alexander Quinn Nichol and Prafulla Dhariwal. 2021. Improved denoising diffusion probabilistic models. In *International conference on machine learning*. PMLR, 8162–8171.
- [25] Muzaffer Özbey, Onat Dalmaz, Salman UH Dar, Hasan A Bedel, Şaban Öztürk, Alper Güngör, and Tolga Cukur. 2023. Unsupervised medical image translation with adversarial diffusion models. *IEEE Transactions on Medical Imaging* 42, 12 (2023), 3524–3539.
- [26] Jialun Peng, Dong Liu, Songcen Xu, and Houqiang Li. 2021. Generating diverse structure for image inpainting with hierarchical VQ-VAE. In *Proceedings of the IEEE/CVF conference on computer vision and pattern recognition*. 10775–10784.
- [27] Ali Razavi, Aaron Van den Oord, and Oriol Vinyals. 2019. Generating diverse high-fidelity images with vq-vae-2. *Advances in neural information processing systems* 32 (2019).
- [28] Xubin Ren, Jiabin Tang, Dawei Yin, Nitesh Chawla, and Chao Huang. 2024. A survey of large language models for graphs. In *Proceedings of the 30th ACM SIGKDD Conference on Knowledge Discovery and Data Mining*. 6616–6626.
- [29] John Schulman, Filip Wolski, Prafulla Dhariwal, Alec Radford, and Oleg Klimov. 2017. Proximal policy optimization algorithms. *arXiv preprint arXiv:1707.06347* (2017).
- [30] Xiao Shen, Quanyu Dai, Fu-lai Chung, Wei Lu, and Kup-Sze Choi. 2020. Adversarial deep network embedding for cross-network node classification. In *Proceedings of the AAAI conference on artificial intelligence*, Vol. 34. 2991–2999.
- [31] Xiao Shen, Shirui Pan, Kup-Sze Choi, and Xi Zhou. 2023. Domain-adaptive message passing graph neural network. *Neural Networks* 164 (2023), 439–454.
- [32] Yan Sun and Jicong Fan. 2024. Mmd graph kernel: Effective metric learning for graphs via maximum mean discrepancy. In *The Twelfth International Conference on Learning Representations*.
- [33] Siram Swetha, Jinyu Yang, Tal Neiman, Mamshad Nayeem Rizve, Son Tran, Benjamin Yao, Trishul Chilimbi, and Mubarak Shah. 2024. X-former: Unifying contrastive and reconstruction learning for mllms. *arXiv preprint arXiv:2407.13851* (2024).
- [34] Jie Tang, Jing Zhang, Limin Yao, Juanzi Li, Li Zhang, and Zhong Su. 2008. Arnetminer: extraction and mining of academic social networks. In *Proceedings of the 14th ACM SIGKDD international conference on Knowledge discovery and data mining*. 990–998.
- [35] Devavrat Tomar, Guillaume Vray, Behzad Bozorgtabar, and Jean-Philippe Thiran. 2023. Tesla: Test-time self-learning with automatic adversarial augmentation. In *Proceedings of the IEEE/CVF conference on computer vision and pattern recognition*. 20341–20350.
- [36] Laurens Van der Maaten and Geoffrey Hinton. 2008. Visualizing data using t-SNE. *Journal of machine learning research* 9, 11 (2008).
- [37] Ashish Vaswani, Noam Shazeer, Niki Parmar, Jakob Uszkoreit, Llion Jones, Aidan N Gomez, Łukasz Kaiser, and Illia Polosukhin. 2017. Attention is all you need. *Advances in neural information processing systems* 30 (2017).
- [38] Petar Veličković, Guillem Cucurull, Arantxa Casanova, Adriana Romero, Pietro Lio, and Yoshua Bengio. 2017. Graph attention networks. *arXiv preprint arXiv:1710.10903* (2017).
- [39] Man Wu, Shirui Pan, Chuan Zhou, Xiaojun Chang, and Xingquan Zhu. 2020. Unsupervised domain adaptive graph convolutional networks. In *Proceedings of the web conference 2020*. 1457–1467.
- [40] Man Wu, Xin Zheng, Qin Zhang, Xiao Shen, Xiong Luo, Xingquan Zhu, and Shirui Pan. 2024. Graph Learning under Distribution Shifts: A Comprehensive

- Survey on Domain Adaptation, Out-of-distribution, and Continual Learning. *arXiv preprint arXiv:2402.16374* (2024).
- [41] Qitian Wu, Hengrui Zhang, Junchi Yan, and David Wipf. 2022. Handling distribution shifts on graphs: An invariance perspective. *arXiv preprint arXiv:2202.02466* (2022).
 - [42] Jiaren Xiao, Quanyu Dai, Xiao Shen, Xiaochen Xie, Jing Dai, James Lam, and Ka-Wai Kwok. 2024. Semi-supervised domain adaptation on graphs with contrastive learning and minimax entropy. *Neurocomputing* 580 (2024), 127469.
 - [43] Keyulu Xu, Weihua Hu, Jure Leskovec, and Stefanie Jegelka. 2018. How powerful are graph neural networks? *arXiv preprint arXiv:1810.00826* (2018).
 - [44] Hongliang Yan, Yukang Ding, Peihua Li, Qilong Wang, Yong Xu, and Wangmeng Zuo. 2017. Mind the class weight bias: Weighted maximum mean discrepancy for unsupervised domain adaptation. In *Proceedings of the IEEE conference on computer vision and pattern recognition*. 2272–2281.
 - [45] Ling Yang, Zhilong Zhang, Yang Song, Shenda Hong, Runsheng Xu, Yue Zhao, Wentao Zhang, Bin Cui, and Ming-Hsuan Yang. 2023. Diffusion models: A comprehensive survey of methods and applications. *ACM computing surveys* 56, 4 (2023), 1–39.
 - [46] Yuning You, Tianlong Chen, Zhangyang Wang, and Yang Shen. 2023. Graph domain adaptation via theory-grounded spectral regularization. In *The eleventh international conference on learning representations*.
 - [47] Zhen Zhang, Meihan Liu, Anhui Wang, Hongyang Chen, Zhao Li, Jiajun Bu, and Bingsheng He. 2024. Collaborate to Adapt: Source-Free Graph Domain Adaptation via Bi-directional Adaptation. In *Proceedings of the ACM on Web Conference 2024*. 664–675.

Received 20 February 2007; revised 12 March 2009; accepted 5 June 2009